05,06

Crystal and electronic structure of the composite compound $Bi_{1-x}La_xFe_{1-y}Mn_yO_{3+\sigma}$ according to X-ray diffraction and X-ray electron spectroscopy

© K.A. Guglev[1], A.T. Kozakov[2], A.G. Kochur[1], A.V. Nikolskii[2], A.G. Rudskaya[3]

[1] Rostov State Transport University,
Rostov-on-Don, Russia
[2] Scientific-Research Institute of Southern Federal University,
Rostov-on-Don, Russia
[3] Southern federal University,
Rostov-on-Don, Russia

E-mail: googlev@rambler.ru, kozakov_a@mail.ru

Received December 24, 2024
Revised December 30, 2024
Accepted December 31, 2024

Based on X-ray photoelectron spectroscopy data, the ratio of the proportions of trivalent and tetravalent manganese Mn^{3+}/Mn^{4+} in the ceramic composite compound $Bi_{1-x}La_xFe_{1-y}Mn_yO_{3+\sigma}$ was determined. Profiles of X-ray photoelectron La3*d*-, La4*d*-, Fe2*p*- and Mn2*p*-spectra were calculated in the isolated ion approximation, taking into account multiplet splitting in the final state of photoionization. Good agreement with experiment was obtained

Keywords: X-ray photoelectron spectroscopy, valence state, mu ltiplet splitting, X-ray diffraction.

DOI: 10.61011/PSS.2025.02.60679.348

1. Introduction

Multiferroics are materials that simultaneously possess magnetic, ferroelectric, and ferroelastic order parameters, with coupling between them [1]. The interest in multiferroics is primarily attributable to the possibility of their practical application. In the case, for example, of the coexistence of ferroelectric and magnetic orders in such materials, it is possible to change the magnetic properties when exposed to polarization by an electric field and vice versa. This property opens up wide prospects for the use of such materials in electronics. Therefore, the study of the features of electric and magnetic systems in multiferroics and their manifestations in various effects important for practical application is an important fundamental scientific task.

The most widely studied multiferroics are oxides with a perovskite structure with the general formula ABO_3. One of the most well-studied compounds of this type by various methods are bismuth ferrite $BiFeO_3$ and lanthanum manganite $LaMnO_3$.

Bismuth ferrite $BiFeO_3$ (BFO) belongs to rhombohedrally distorted perovskites (symmetry group $R3c$); it has an electric dipole long-range ordering at room temperature [2–5]. Its ferroelectric properties are preserved at temperatures, according to various data, up to $T_c \approx 1103$ K [6], or $T_c \approx 1123$ K [7]. However, the spiral magnetic ordering of ions Fe^{3+} in the direction [111] persists at significantly lower temperatures, $T_N \approx 640$ K [8].

The valence state of iron ions in BFO (bismuth ferrite) and related compounds doped with divalent barium, calcium, or strontium ions was a subject of debate [9–11], until it was rigorously demonstrated in Ref. [12] that BFO contains exclusively trivalent iron, provided no oxygen vacancies are present in the material's crystal structure. In cases where oxygen vacancies appeared in the crystal structure of BFO, Fe^{2+} ions were detected in the samples, as evidenced by characteristic changes in the X-ray photoelectron Fe2*p*-spectrum [9].

Lanthanum manganite $LMnO_3$ (LMO), is characterized at room temperature by either orthorhombic phases (*Pnma* or *Pbnm*) or rhombohedral phase $R3c$ depending on the type and concentration of defects. $LaMnO_3$ is both an insulator and an antiferromagnet [13] due to the superexchange bond between ions Mn^{3+}, and the value of its temperature T_N is ≈ 480 K [14–16].

At the same time, numerous solid solutions based on $LaMnO_3$ not only exhibit properties characteristic of multiferroics, but also possess tremendous magnetoresistance. The valence state of manganese ions in LMO and related compounds obtained by partial substitution of trivalent lanthanum with either trivalent bismuth ions $La_{1-x}Bi_xMnO_3$ or divalent ions $La_{1-x}B_xMnO_3$ ($B = Ca, Sr, Ba$) has also been the subject of extensive discussions [11,17]. The effect of temperature on the valence state of manganese was established in Ref. [18] using $YMnO_3$ as an example: heat treatment of a sample initially containing only Mn^{3+} ions led to the appearance of additional Mn^{4+} ions in the crystal lattice.

The heterostructure of BFO/LMO is another unique compound [19,20]. The authors showed in Ref. [19] that

BFO/LMO composite compounds contain phase-separated compounds $BiFeO_3$ and $LaMnO_3$. The phase $BiFeO_3$ phase has a rhombohedral structure $R3c$, and the phase $LaMnO_3$ has a rhombic structure $Pnma$. The $Pnma$ structure exhibits a slight reduction in lattice cell size in the BFO/LMO composite materials. The valence state of Fe and Mn ions in BFO/LMO composite compounds was also studied by X-ray photoelectron spectroscopy in Refs. [19,20]. The authors disputed the possibility of an excessive magnetic moment caused by the coexistence of charge states Fe^{2+}/Fe^{3+} or Mn^{3+}/Mn^{4+} due to the formation of oxygen vacancies. According to their findings, Mn and Fe ions in the BFO/LMO compound exist exclusively in the 3+ charge state [19,20].

It is generally assumed that the unique properties of multiferroics with a perovskite structure, which include a rare earth element and a transition metal, are attributable in whole or in part to the local magnetic moments of ions with $3d$- (transition metals), $4f$- and $5f$- (rare earth elements) shells and their interaction with collectivized electrons of the outer shells. This understanding explains the growing interest in studies investigating the nature of this phenomenon, particularly regarding the valence states of manganese and iron and their role in the unique properties of these materials. Given the lack of a unified theory describing the properties of such materials, determining the valence states of manganese and iron ions in BFO, LMO, and their derived compounds remains a crucial and timely research challenge. Our previous studies of iron-containing [10,12] and manganese-containing [11,17,21] multiferroics demonstrated the possibility of determining the valence state of transition metal ions using Fe2p- and Mn2p-X-ray photoelectron spectra.

The purpose of this paper is to study the crystal structure, elemental composition, and valence state of the cations of the composite compound $Bi_{1-x}La_xFe_{1-y}Mn_yO_{3+\sigma}$ by X-ray electron spectroscopy and X-ray diffraction.

2. Experimental part

2.1. Sample preparation

Sample of $Bi_{1-x}La_xFe_{1-y}Mn_yO_{3+\sigma}$ was prepared by two-stage solid-phase synthesis from a stoichiometric mixture of oxides Bi_2O_3, Fe_2O_3, La_2O_3, Mn_2O_3 (chemical purity of all oxides not less than 99.9 %) at temperatures of $T_1 = 750\,^\circ$C ($\tau = 4$ h) and $T_2 = 950\,^\circ$C ($\tau = 4$ h).

2.2. X-ray diffraction data

X-ray diffraction data were acquired using Rigaku Ultima IV diffractometer with filtered Cu-$K_\alpha$radiation with θ-2θ-scanning in the angle range of $20 \le 2\theta \le 60^\circ$. The structure refinement was performed using the Rietveld full-profile method with the FullProf software, employing a pseudo-Voigt function for peak fitting.

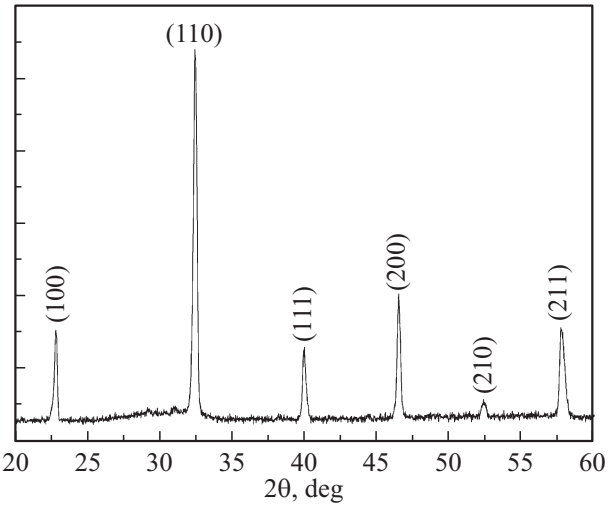

Figure 1. Fragment of the X-ray diffraction profile of a ceramic sample of $Bi_{1-x}La_xFe_{1-y}Mn_yO_{3+\sigma}$ at room temperature. The Miller indices are given for the cubic phase Pn-3m.

The X-ray diffraction profile of a ceramic sample of $Bi_{1-x}La_xFe_{1-y}Mn_yO_{3+\sigma}$ was analyzed at room temperature. As evidenced by the shape and splitting of XRD reflections (Figure 1), the sample $Bi_{1-x}La_xFe_{1-y}Mn_yO_{3+\sigma}$ crystallizes in a cubic phase with space group Pm-3m (No. 221). All reflections are single, and correspond to the cubic perovskite phase characteristic of the high-temperature lanthanum manganite phase.

Cubic cell parameters $a = 3.910$ Å ($\Delta a = 0.001$ Å), $V = 59.75$ Å^3 ($\Delta V = 0.02$ Å^3). Positions of atoms (in cell fractions): Bi/La (1a: 0, 0, 0); Fe/Mn (1b: 0.5, 0.5, 0.5); O (3c: 0.5, 0.5, 0).

Since the experimental volume of the cell $Bi_{1-x}La_xFe_{1-y}Mn_yO_{3+\sigma}$ is less than the cell volume for pure $BiFeO_3$, but greater than the volume of pure $LaMnO_3$, $62.45 > 59.75 > 58.57$ Å^3, it can be argued that La^{3+} and Mn^{3+} ions are embedded in the cationic A and B sublattices of bismuth ferrite, replacing ions Bi^{3+} and Fe^{3+}.

2.3. X-ray photoelectron spectroscopy data

Preparation of the surface of the test sample $Bi_{1-x}La_xFe_{1-y}Mn_yO_{3+\sigma}$ for X-ray photoelectron spectroscopy studies was performed by mechanical scraping with a diamond scraper at a pressure of 10^{-6} Pa in the preparation chamber of the analyzer. Spectra of internal levels Fe2p-, Mn2p-, La4d-, La3d-, Bi4f-, O1s- and C1s-were acquired using monochromated AlK_α X-ray radiation with an energy of 1486.6 eV using a surface analysis system ESCALAB 250 with X-ray microprobe. The size of the X-ray spot on the sample was 500 μm. The spectra were acquired in 0.1 eV increments. The positive charge of the sample during spectral measurements was corrected by additional irradiation of the sample surface with slow electron beams. The bond energy scales of the XPS spectra

were calibrated relative to the carbon line C1*s*, the bond energy of which was assumed to be 285 eV.

The elemental composition of the samples was determined from the intensities of the Mn2*p*-, Fe2*p*-, La4*d*-, Bi4*f*- and O1*s* X-ray photoelectron lines using the ESCALAB 250 system software. The following procedure was used to determine the atomic concentrations taking into account the presence of several components in the intensity of the analytical line O1*s*. A series of element concentrations were determined for each sample with fixed input intensities of the Mn2*p*, Fe2*p*, La4*d*, Bi4*f* lines and different intensities of the main component of the O1*s* line, corresponding to oxygen incorporated into the sample's crystal lattice.

The concentrations of the elements were calculated employing the standard approach [22,23] using the ratio:

$$C_i(\text{at.}\%) = \frac{I_i/\left(I_i^{\infty}T(E_i)\right)}{\Sigma_j I_j/\left(I_j^{\infty}T(E_j)\right)} \times 100\,\%. \qquad (1)$$

Here I_i are the integral intensities of the analytical lines of the XPS, and I_i^{∞} is the empirically acquired atomic sensitivity coefficients for the XPS [24], $T \sim E_{\text{kin}}^{-1/2}$ is the hardware coefficient, which takes into account the dependence of the transmittance coefficient of the energy analyzer on the electron kinetic energy [23,24]. The background was subtracted using the Shirley method [22].

The profiles Mn2$p_{3/2,1/2}$ of the X-ray photoelectron spectra show that the studied samples contain manganese ions of different charges: Mn^{3+} and Mn^{4+} [11,21,25]. We determined the relative fractions of Mn^{3+}/Mn^{4+} ions in the samples using the Mn2$p_{3/2,1/2}$ spectral profiles and following the methodology in Refs. [26,27]. The method for determining the relative proportions of ions is described in the next section. Knowledge of atomic concentrations and ion charges made it possible to determine the charge balance Δ_{el}, i.e., the sum of the charges of all cations (Bi^{3+}, Fe^{3+}, La^{3+}, Mn^{3+} and Mn^{4+}) and anions (O^{2-}) in the structural unit of the sample. Figure 2, *a, b, c* shows the calculated dependences of element concentrations on the oxygen nonstoichiometry parameter σ for the sample of $Bi_{1-x}La_xFe_{1-y}Mn_yO_{3+\sigma}$. Figure 2, *c* shows the dependence of the balance of charge Δ_{el} on σ.

According to the method proposed in Refs. [26,27], the elemental composition of the sample is determined for a value σ at which the structural unit of the sample is electrically neutral. The requirement for the electroneutrality of the sample is satisfied if, in Figure 2, *c*, the value σ is selected, which corresponds to $\Delta_{\text{el}} = 0$ (point N in Figure 2, *c*). A vertical straight line passing through the point N will cross the graphs of Mn, Fe, and Bi concentrations; these intersection points give the desired concentrations of the elements. The ion concentrations calculated in this way for the samples studied in this study are shown in the following table.

Ion concentrations and formula composition of the sample of $Bi_{1-x}La_x$ $Fe_{1-y}Mn_yO_{3+\sigma}$ acquired from the electron neutrality condition of the sample (XPS)

Sample	$Bi_{1-x}La_xFe_{1-y}Mn_yO_{3+\sigma}$				
	La	Bi	Mn	Fe	O
Concentration, at.%	8.16	17.43	12.31	2.87	59.23
Formular composition	$Bi_{17.43}La_{8.16}Fe_{2.87}Mn_{12.31}O_{59.23}$				

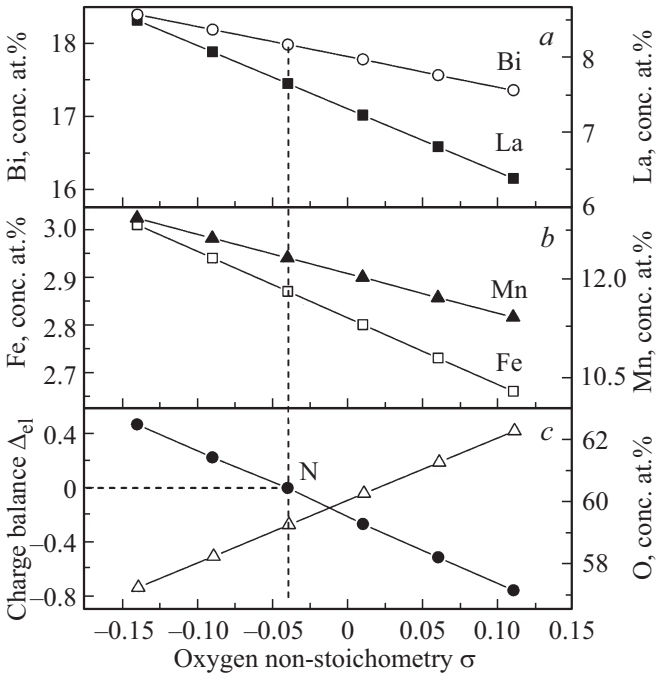

Figure 2. Element concentrations calculated for the sample of $Bi_{1-x}La_xFe_{1-y}Mn_yO_{3+\sigma}$ and the total charge Δ_{el} of all ions in the structural unit of the compound at different values of the nonstoichiometry parameter σ. The concentrations of elements in the sample were determined with $\Delta_{\text{el}} = 0$. The corresponding nonstoichiometry parameter $\sigma = -0.04$.

3. Results and discussion

Figure 3 shows the X-ray photoelectron spectra of levels O1*s* and Bi4*f* in the sample of $Bi_{17.43}La_{8.16}Fe_{2.87}Mn_{12.31}O_{59.23}$ after background subtraction. It can be seen that the spectrum of the 1*s*-level of oxygen has two components, designated as A-529.4 eV and B-531 eV. The component with a bond energy of 529.4 eV is attributed to oxygen in the crystal lattice of the studied compound. The components with a bond energy of 531 eV belong to the adsorbed oxygen or OH groups [28–31].

The spectrum of Bi4*f* is a doublet consisting of two peaks of Bi4$f_{7/2}$ and Bi4$f_{5/2}$ separated by an energy interval of 5.2 eV due to spin-orbit splitting of the 4*f*-level. The more intense Bi4$f_{7/2}$ line has a bond energy of

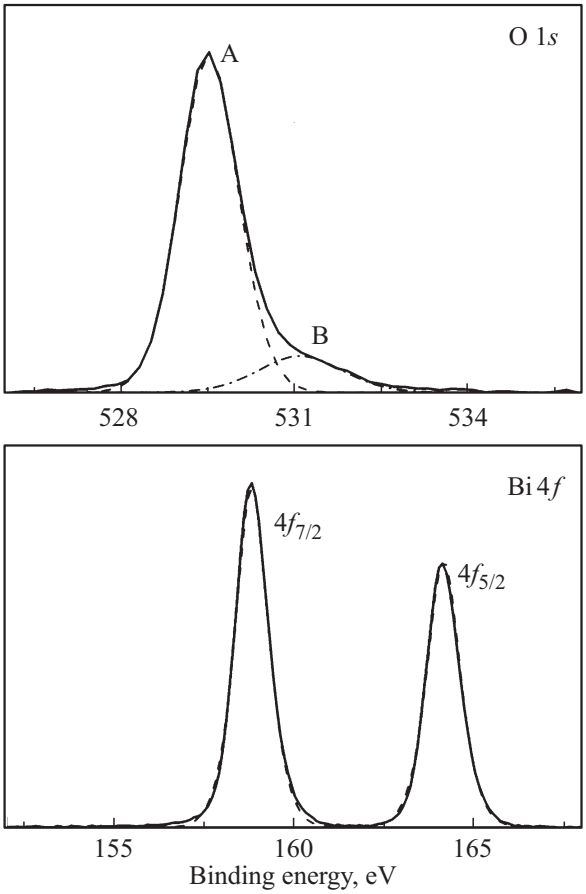

Figure 3. Bi4f- and O1s are X-ray photoelectron spectra of a composite sample of $Bi_{17.43}La_{8.16}Fe_{2.87}Mn_{12.31}O_{59.23}$.

158.8 eV, and the less intense Bi4$f_{5/2}$ peak has a bond energy of 164 eV. Such bond energy values are characteristic of bismuth bound to oxygen in the crystal lattice and correspond to Bi in the trivalent state [23].

Figure 4, *a, b* show La4d and La3d spectra of sample of $Bi_{17.43}La_{8.16}Fe_{2.87}Mn_{12.31}O_{59.23}$ and on the panel with La3d spectrum for La_2O_3 compound [21]. La4d is the X-ray photoelectron spectrum shown in Figure 4, *a*, constitutes a spin doublet. The more intense La4$d_{5/2}$ line has a bond energy of 102 eV, and the less intense La4$d_{3/2}$ line has a bond energy of 104.9 eV. The vertical bars represent the calculation results for La^{3+} ion.

The experimental La3d spectrum of the studied $Bi_{17.43}La_{8.16}Fe_{2.87}Mn_{12.31}O_{59.23}$ compound (circles) shown in Figure 4, *b* is compared with the spectrum of La^{3+} ion calculated in Ref. [21] taking into account charge transfer satellites. It can be seen that the calculated La3d-spectrum reproduces well the main features of the experimental spectrum. It should be also noted that La3d-spectrum for $Bi_{17.43}La_{8.16}Fe_{2.87}Mn_{12.31}O_{59}$ acquired in this study, agrees well with the spectra of La_2O_3 and $Bi_{0.17}La_{0.54}Mn_{0.88}O_{3.40}$ compounds acquired earlier in Ref. [21], in which lanthanum is in the trivalent state. The spectrum of La_2O_3 is reproduced in Figure 4, *c*.

These data allow drawing a conclusion that lanthanum in $Bi_{17.43}La_{8.16}Fe_{2.87}Mn_{12.31}O_{59.23}$ compound is in a charge state 3+.

Figure 5, *a* shows the experimental X-ray electron Fe2p-spectrum acquired from the surface of the $Bi_{17.43}La_{8.16}Fe_{2.87}Mn_{12.31}O_{59.23}$ composite compound. It can be seen from Figure 5, *a* that the experimentally acquired X-ray photoelectron spectrum of 2p-level of the iron level for the sample of $Bi_{17.43}La_{8.16}Fe_{2.87}Mn_{12.31}O_{59.23}$ has two maxima A and C corresponding to Fe2$p_{3/2}$ and Fe2$p_{1/2}$, spin-doublet levels, as well as charge transfer satellites designated B and D. The main maximum of the A-Fe2$p_{3/2}$ spectrum for the $Bi_{17.43}La_{8.16}Fe_{2.87}Mn_{12.31}O_{59.23}$ compound has an energy of 710.5 eV. This is the value of the bond energy, and most importantly, the presence of a characteristic charge transfer satellite B at a distance of 8.3 eV from the main line A correspond to the iron ion in the trivalent state.

Figure 5, *b* shows the experimental X-ray electron 2p-spectrum of a single crystal of $PbFe_{1/2}Nb_{1/2}O_3$ in which iron ions are in the trivalent state. 2p-spectra of $Bi_{17.43}La_{8.16}Fe_{2.87}Mn_{12.31}O_{59.23}$ and $PbFe_{1/2}Nb_{1/2}O_3$ are

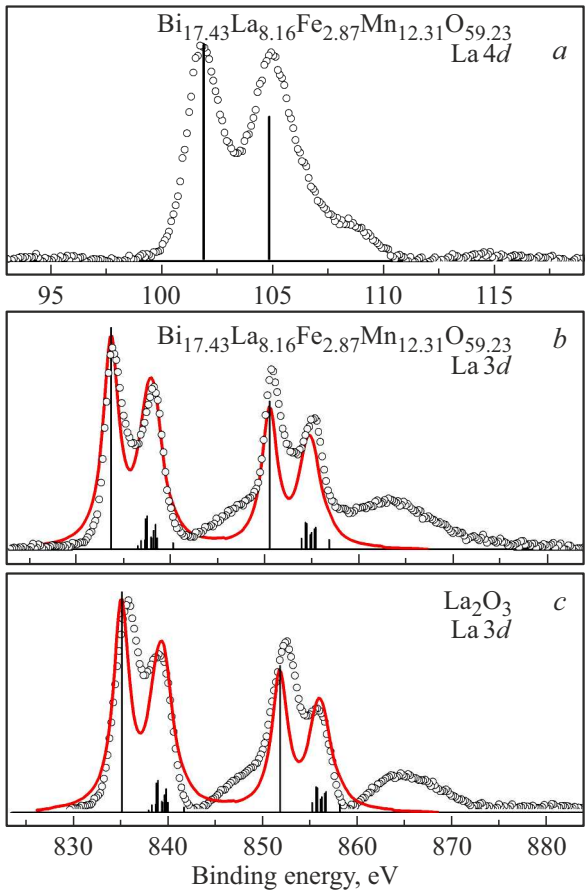

Figure 4. Spectra of La3d-, La4d-levels for $Bi_{17.43}La_{8.16}Fe_{2.87}Mn_{12.31}O_{59.23}$ composite compound and spectrum of La3d-level for La_2O_3 compound [21]. Experimental data are shown by circles, calculated data are shown by columns and a solid line.

compared in Figure 5 with the Fe2*p*-spectrum of Fe^{3+} ion calculated in Ref. [12]. The calculation in Ref. [12] takes into account the spin-orbital splitting of the 2*p*-level, multiplet splitting due to the interaction of electrons of 3*d*-subshell with a 2*p*-vacancy, charge transfer satellites and level splitting due to the crystal field of the atoms of the environment in octahedral coordination. The good match of the acquired 2*p*-spectrum with the calculation and agreement with the shape of the Fe2*p*-spectrum of the trivalent iron for a single crystal of $PbFe_{1/2}Nb_{1/2}O_3$ confirm the conclusion that iron ions in the $Bi_{17.43}La_{8.16}Fe_{2.87}Mn_{12.31}O_{59.23}$ compound are in the state Fe^{3+}.

Figure 6 shows the experimental Mn2*p*-spectrum of the $Bi_{17.43}La_{8.16}Fe_{2.87}Mn_{12.31}O_{59.23}$ compound and results of its decomposition into components corresponding to 2*p*-spectra of Mn^{3+} and Mn^{4+} ions. $Mn_2O_3(Mn^{3+})$ and $SrMnO_3$ (Mn^{4+}) spectra were used as basis spectra for spectral decomposition, with both spectra normalized to identical total intensity. Experimental profiles of Mn2*p*-spectra in Mn_2O_3 with trivalent manganese ion and $SrMnO_3$ with trivalent manganese ion were acquired in Refs. [11,21,25].

The spectrum was adjusted in a spectral region that captures only the $Mn2p_{3/2}$ peak, nevertheless, a good correspondence of the synthesized spectrum to the experimental one was acquired over the entire spectral range. It should also be noted that no restrictions were imposed on the optimized contributions when optimizing the contributions of the spectra of trivalent and tetravalent Mn ions. At the same time, the sum of the optimal contributions of Mn^{3+} and Mn^{4+} spectra turned out to be equal to 1, which indicates the sufficient reliability of the procedure used.

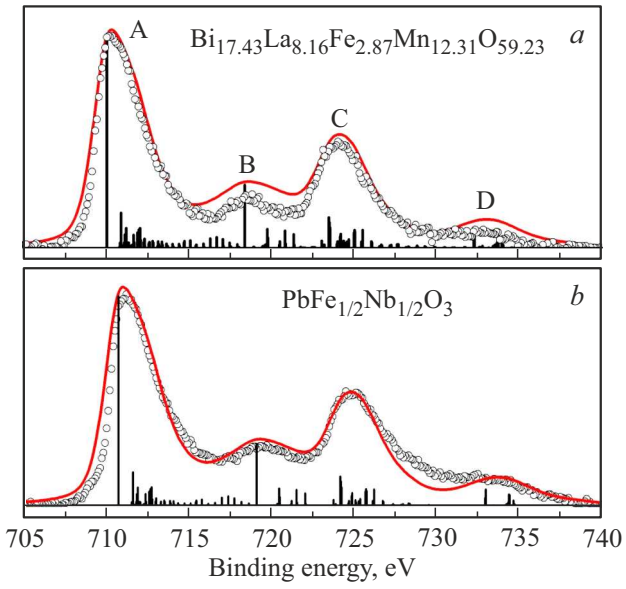

Figure 5. Fe2*p*-level spectra for $Bi_{17.43}La_{8.16}Fe_{2.87}Mn_{12.31}O_{59.23}$ composite compound and single crystal of $PbFe_{1/2}Nb_{1/2}O_3$. Experimental data are shown by circles, calculated data for Fe^{3+} ion are shown by columns and a solid line [12].

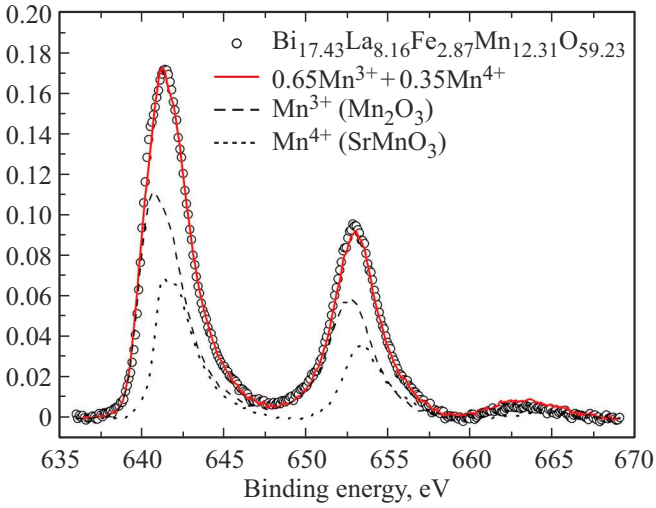

Figure 6. Experimental Mn2*p*-spectrum of sample of $Bi_{17.43}La_{8.16}Fe_{2.87}Mn_{12.31}O_{59.23}$ (circles) and superposition of 2*p*-spectra of $Mn_2^{3+}O_3$ and $SrMn^{4+}O_3$ (solid line). The dashed and dotted lines show the contributions of components Mn^{3+} and Mn^{4+}, respectively.

The fractions of trivalent and tetravalent manganese ions for $Bi_{17.43}La_{8.16}Fe_{2.87}Mn_{12.31}O_{59.23}$ compound acquired as a result of spectrum decomposition were 0.65 and 0.35, respectively.

4. Conclusion

$Bi_{17.43}La_{8.16}Fe_{2.87}Mn_{12.31}$ $O_{59.23}$ compound was synthesized. The lattice cell parameters were studied by X-ray diffraction. The elemental composition determined by X-ray photoelectron spectroscopy shows a slight oxygen deficiency of $\sigma = -0.04$ the presence in the sample of $Bi_{17.43}La_{8.16}Fe_{2.87}Mn_{12.31}O_{59.23}$. Analysis of the profile of the Fe2*p*-spectrum showed the presence of only trivalent iron in the sample. At the same time, the analysis of the profile of the Mn2*p* spectrum showed the presence of both trivalent and tetravalent ions in the sample. The fractions of Mn^{3+} and Mn^{4+} ions are 0.65 and 0.35.

Funding

The study was supported by the Ministry of Science and Higher Education of the Russian Federation (State assignment in the field of scientific activity for 2023 No. FENW-2023-0014).

Conflict of interest

The authors declare no conflict of interest.

References

[1] W. Eerenstein, N.D. Mathur, J.F. Scott. Nature. **442** (17), 759-765 (2006).
[2] J. Li, Y. Duan, H. He, D. Song. J. Alloys Compd. **315**, 259–264 (2001).
[3] V.I. Torgashev, A.A. Volkov, A.A. Bush, E.S. Zhukova, S.N. Migunov, A.N. Lobanov, B.P. Gorshunov. Phys. Solid State **49**, 1652 (2007).
[4] A.J. Jacobson, B.E.F. Fender. J. Phys. C.: Solid State Phys. **8**, 844 (1975).
[5] P. Fisher, M. Polomska, I. Sosnowska, M. Szymanski. J. Phys. C.: Solid State Phys. **13**, 1931 (1980).
[6] C. Michel, J.M. Moreau, G.D. Achenbach, R. Gerson, W.J. James. Solid State Commun. **7**, 701–7 (1969).
[7] I. Sosnowska, R. Przenioslo, P. Fischer, V.A. Murashov. J. Magn. Magn. Mater. **160**, 384–385 (1996).
[8] A. Biran, P.A. Montano, U. Shimony. J. Phys. Chem. Sol. **32**, 327 (1971).
[9] A. Kania, E. Talik, M. Kruczek. Ferroelectrics **391**, 114 (2009).
[10] A.T. Kozakov, A.G. Kochur, V.I. Torgashev, A.A. Bush, V.Ya. Shkuratov, S.P. Kubrin, A.V. Nikolskii, K.A. Googlev. J. Electron Spectros. Relat. Phenomena **189**, 106 (2013).
[11] A.T. Kozakov, A.G. Kochur, K.A. Googlev, A.V. Nikolskii, V.I. Torgashev, V.G. Trotsenko, A.A. Bush. J. Alloys Compd. **647**, 947 (2015)
[12] A.T. Kozakov, A.G. Kochur, K.A. Googlev, A.V. Nikolsky, I.P. Raevski, V.G. Smotrakov, V.V. Eremkin. J. Electron Spectros. Relat. Phenomena **184**, 16–23 (2011).
[13] Y.D. Zhao, J. Park, R.-J. Jung, H.-J. Noh, S.-J. Oh. J. Magn. Magn. Mater. **280**, 404 (2004).
[14] B.R.K. Nanda, S. Satpathy. Phys. Rev. B **79**, 054428 (2009).
[15] S. Dong, R. Yu, S. Yunoki, G. Alvarez, J.-M. Liu, E. Dagotto. Phys. Rev. B **78**, 201102(R) (2008).
[16] S. Smadici, P. Abbamonte, A. Bhattacharya, X. Zhai, B. Jiang, A. Rusydi, J.N. Eckstein, S.D. Bader, J.-M. Zuo. Phys. Rev. Lett. **99** (2007).
[17] A.G. Kochur, A.T. Kozakov, A.V. Nikolskii, K.A. Googlev, A.V. Pavlenko, I.A. Verbenko, L.A. Reznichenko, T.I. Krasnenko. J. Electron Spectros. Relat. Phenomena **185**, 175 (2012).
[18] A.G. Kochur, A.T. Kozakov, K.A. Googlev, A.V. Nikolskii. Journal of Electron Spectroscopy and Related Phenomena **195**, 1–7 (2014).
[19] Abdelilah Lahmar, Salah Habouti. Claus-Henning Solterbeck, Mohammed Es-Souni, Brahim Elouadi. J. Appl. Phys. **105**, 014111 (2009).
[20] Shreeja Pillai, Deepika Tripathi, Touseef Ahmad Para, Amitabh Das, T. Shripathi, Vilas Shelke. J. Appl. Phys. **120**, 164103 (2016).
[21] A.T. Kozakov, A.G. Kochur, L.A. Reznichenko, L.A. Shilkina, A.V. Pavlenko, A.V. Nikolskii, K.A. Googlev, V.G. Smotrakov. J. Electron Spectros. Relat. Phenomena **186**, 14 (2013).
[22] D. Briggsand, M.P. Seach (Eds.), Practical Surface Analysis by Auge rand X-Ray Photoelectron Spectroscopy, John Wiley & Sons, Chichester, (1983). 533 p.
[23] V.I. Nefedov. Rentgenovskaya fotoelektronnaya spektroskopiya khimicheskikh soedinenij, Khimiya, Moskva, (1984), p. 256. (in Russian).
[24] C.D. Wagner, W.M. Riggs, L.E. Davis, J.F. Moulder (Eds.). Handbook of X-Ray Photoelectron Spectroscopy. Perkin–Elmer Corporation (1979). 190 p.
[25] A.T. Kozakov, A.G. Kochur, V.G. Trotsenko, A.V. Nikolskii, M. El Marssi, B.P. Gorshunov, V.I. Torgashev. J. Alloys Compd. **740**, 132 (2018).
[26] N.A. Liedienov, Z. Wei, V.M. Kalita, A.V. Pashchenko, Q. Li, I.V. Fesych, V.A. Turchenko, C. Hou, X. Wei, B. Liu, A.T. Kozakov, G.G. Levchenko. Appl. Mater. Today **26**, 101340 (2022).
[27] A.T. Kozakov, A.G. Kochur, A.V. Nikolskii, I.P. Raevski, S.P. Kubrin, S.I. Raevskaya, V.V. Titov, A.A. Gusev, V.P. Isupov, G. Lid, I.N. Zakharchenko. J. Electron Spectros. Relat. Phenomena **239**, 146918 (2020).
[28] A. Fujimori, M. Saeki, N. Kimizuka, M. Taniguchi, S. Suga. Phys. Rev. B **34**, N10, 7318–7328 (1986)
[29] E. Begreuther, S. Grafström, L.M. Eng, C. Thiele, K. Dörr. Phys. Rev. B **73**, 155425 (2006)
[30] A.E. Bocquet, A. Fujimori, T. Mizokawa, T. Saitoh, H. Namatame, S. Suga, N. Kimizuka, Y. Takeda, M. Takano. Phys.Rev. B **45**, 1561 (1992).
[31] T. Yamashita, P. Hayes. Appl. Surf. Sci. **254**, 2441–2449 (2008).

Translated by A.Akhtyamov